

Synthesis, Characterization, Pharmacogenomics, and Molecular Simulation of Pyridinium Type of Ionic Liquids and Their Applications

Ramalingam Tamilarasan, Kivilvelu Ganesan,* Annadurai Subramani, Liyakath Benazir Ali, Mohammed Mujahid Alam, and Amanullah Mohammed



Cite This: *ACS Omega* 2023, 8, 4146–4155



Read Online

ACCESS |



Metrics & More

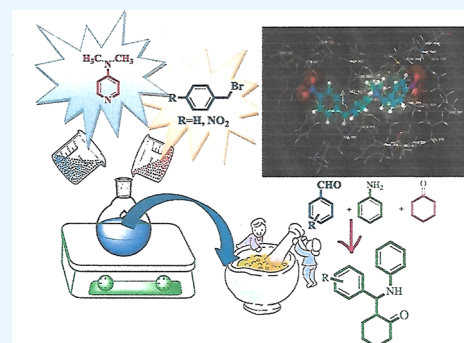


Article Recommendations



Supporting Information

ABSTRACT: Substituted pyridinium bromides are prepared by conventional and solvent-free greener methods. The solvent-free solid-phase (greener) method is superior to the conventional method because of its nontoxic nature, simple reaction setup procedure, and twenty times less time consumption. Column chromatography and toxic organic solvents are avoided. Substituted pyridinium salts 1–2(a–c) show excellent catalytic response in the preparation of β -amino carbonyl derivatives using the conventional approach. Pharmacokinetics is very important in target validation and in shifting a lead compound into a drug. The physicochemical properties discussed here can be used effectively in the drug designing candidate, which is a cumbersome process in clinical research. In addition, molecular simulations are demonstrated, and compounds 1–2(a–c) possess the most potent VEGFR-2 kinase protein inhibitory activities, and most interestingly, compound 2a strongly binds and regulates the VEGFR-2 kinase activity in therapeutic approaches and cancer prevention.



1. INTRODUCTION

Ionic liquids (ILs) have earned themselves a reputation as excellent reaction media. Earlier applications of ILs were mainly as electrolytes, solvents, and extractants. The scope of their application is now broader and covers their use as reaction media, fuel cells, optical fluids, solar cells, energetic materials, heat transfer fluids, and lubricants, to name only a few.¹ The properties of imidazolium/pyridinium salt are varied with different counter anions, which can enhance or suppress the catalytic activities.^{2–5} Pyrazole and its derivatives have emerged as important compounds among the other heterocyclic compounds due to their medicinal properties like anti-inflammatory,^{6,7} analgesic,^{8,9} antimicrobial,¹⁰ anticancer,¹¹ antiviral,¹² antipyretic,¹³ and antianxiety activities,¹⁴ and some of the reports proved that adding other materials like nitrogen-containing phosphane^{15,16} and ligands^{17,18} to pyrazolium/pyridinium^{19,20} and imidazolium^{21–24} can give more stability to the compound, which are recyclable catalytic moieties. The drug discovery and evolution process aims at finding a compound, possessing good pharmacodynamic and pharmacokinetic properties. It is eminent that drugs designed can be more productive if physicochemical properties are carefully analyzed and applied in a defined way during development. The early prediction of ADME properties in the drug-designing phase considerably diminishes the fraction of pharmacokinetics-related failures in clinical trials.²⁵ The proposed set of

compounds is optimized by virtual ADME screening by the tool SwissADME.

Synthesized protic ILs in the form of 1-alkyl- and 1-alkoxymethylimidazolium lactates found that antimicrobial activities of the protic ILs are strongly related to the length of the substituent and the type of anion. Anthracene-linked trimeric imidazolium bromide is prepared by the conventional approach.²⁶ Trimeric imidazolium salt formed an excellent selective sensor for picric acid.²⁷ Dimeric, trimeric, and tetrameric pyridinium cations with a bromide counter anion played a crucial role in detecting various anions in an aqueous environment.²⁸ Host–guest interaction is involved between β -cyclodextrin and alkyl/aryl-substituted dimeric imidazolium salt in a kneading approach.²⁹

In the present work, we have synthesized quaternary ammonium-based pyridinium salts under conventional/solvent-free silica-supported conditions as well as their catalytic properties, which are described here. Using the conventional/solid-phase approach, we investigated one-spot preparation of β -

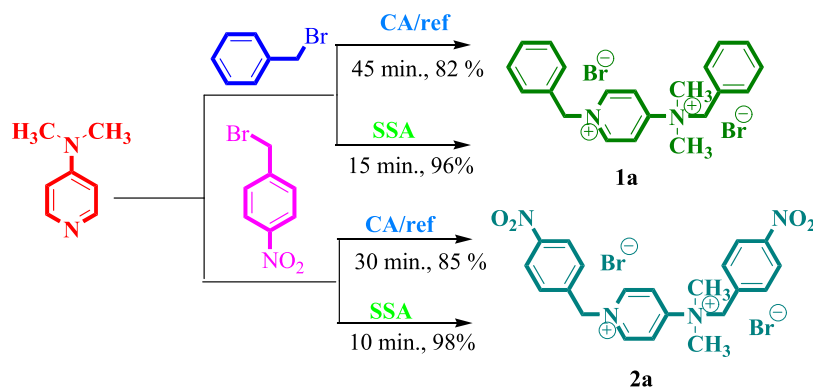
Received: November 4, 2022

Accepted: December 22, 2022

Published: January 16, 2023



Scheme 1. Synthesis of Benzyl/4-Nitrobenzyl-Substituted Quaternary Ammonium-Based Pyridinium Bromide Using Multiple Approaches^a



^aReagent and conditions: Conventional approach (CA): CH₃CN, ref, 30–45 min, 82–85%; Solid-supported approach (SSA): Muffle furnace, 100 °C, 10–15 min, 96–98%.

amino carbonyl derivatives with the optimal concentration of our synthesized pyridinium salts. The preparation of β -amino carbonyl derivatives with our catalyst is substantially more effective, to the best of our knowledge, based on the literature. Furthermore, we explored the molecular modeling and binding affinities of quaternary ammonium-based pyridinium type of ionic liquids as pharmacological molecules against various macromolecular receptors, such as H-bonding, π - π stacking, salt bridge, and hydrophobic contacts.

2. RESULTS AND DISCUSSION

Synthesis of benzyl/4-nitrobenzyl-substituted pyridinium bromide **1a/2a** from *N,N*-dimethyl pyridine-4-amine (1.853×10^{-3} mmol; 1.0 equiv) is treated with benzyl/4-nitrobenzyl bromide (1.65×10^{-2} mmol; 2.05 equiv) in the presence of 20 mL of dry CH₃CN under refluxing conditions for 30–45 min to give benzyl/4-nitrobenzylated pyridinium bromide **1a/2a** in quantitative yield. To reduce the toxicity of the *N*-alkylation reaction, it is tried using a solvent-free silica-supported approach under muffle furnace conditions, which is completed in lesser reaction time with higher yield (Scheme 1).

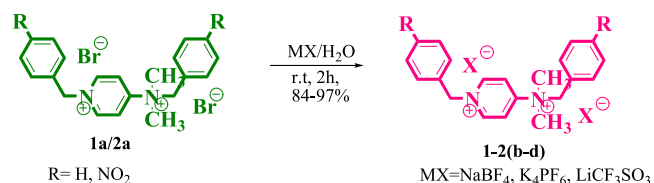
N-alkylation reaction by the solvent-free silica-supported approach is much superior to the conventional approach because of its nontoxicity, shorter reaction time with higher yield, and easy work up. 4-Nitrobenzyl bromide reacts much faster than benzyl bromide due to the weaker C-Br bond in 4-nitrobenzyl bromide.

An anion exchange reaction is carried out with substituted quaternary ammonium-based pyridinium bromide **1a/2a** in the presence of different counter anions containing inorganic salts, such as K₄PF₆, NaBF₄, and LiCF₃SO₃, in the presence of 20 mL of deionized water at room temperature with stirring for 2 h to give anion exchange products of compounds **1–2(b–d)** in 94–98% yield (Scheme 2).

3. CATALYTIC ACTIVITY

We have tried the Mannich reaction using a catalytic amount of benzyl/4-nitrobenzyl-substituted pyridinium salts with and without solvent. 4-Nitrobenzyl-substituted pyridinium bromide **2a** showed excellent catalytic activity than the others. To optimize the catalytic concentration of substituted quaternary ammonium-based pyridinium salts, the reaction is carried out with various concentrations, such as 3.608×10^{-5} , 7.217×10^{-5} , and 1.082×10^{-4} mmol. Among these concentrations, $1.082 \times$

Scheme 2. Preparation of Different Counteranions Containing Quaternary Ammonium-Based Pyridinium Salts



10^{-4} mmol showed excellent catalytic response than the others. While increasing the concentration, there is no appreciable change in the reaction. So, 1.082×10^{-4} mmol concentration is the optimum concentration to prepare β -amino carbonyl compounds.

Various β -amino carbonyl derivatives are prepared by conventional and solvent-free silica-supported approaches, which are catalyzed by benzyl/4-nitrobenzyl quaternary ammonium-based pyridinium salts. The results are summarized in Tables 1 and 2 and compared the catalytic efficiency with available literature reports.³⁰ Senapak and co-workers prepared β -amino carbonyl derivatives³¹ in the presence of an acidic ionic polymer bearing imidazolium type of catalyst required nearly 24 h for completion of the reaction. When comparing the catalytic response between compounds **1a** and **2a**, compound **2a** showed excellent catalytic response even in very low concentrations. After examining the literature reports, compound **2a** is superior to the available reports due to its shorter reaction period, solvent-free, nontoxicity, higher yield, and environmentally friendly nature (Scheme 3).

We have tried the catalytic efficiency of 4th cycle benzyl/4-nitrobenzyl quaternary ammonium-based pyridinium salt in the preparation of β -amino carbonyl compound. Even in the 4th cycle, the product obtained was the same as observed in the fresh use shown in Figure 1.

3.1. Molecular Modeling. A molecular simulation study is an attractive scaffold to understand the ionic liquid–protein interactions, which can corroborate our experimental results. The best interaction site of compounds with target protein is visualized in Figures 2 and 3, and data are summarized in tables. The observed docking score value of compounds **1–2(a–d)** reveals -4.14 , -6.41 , -4.34 , -4.15 , -4.571 , -5.742 , -5.442 , and -5.927 kcal/mol. The docking score results revealed that all compounds are well located in the hydrophobic site and strongly

Table 1. Preparation of β -Amino Carbonyl Derivative Catalyst by Benzyl-Substituted Quaternary Ammonium-Based Pyridinium Salts 1(a–d)

s. no	catalyst	β -amino carbonyl derivatives	Concentration of benzyl quaternary ammonium-based pyrazolium salts											
			4.308×10^{-5} mmol				8.616×10^{-5} mmol				1.292×10^{-4} mmol			
			CA		SSA		CA		SSA		CA		SSA	
time (h:m)	yield %	time (h:m)	yield %	time (h:m)	yield %	time (h:m)	yield %	time (h:m)	yield %	time (h:m)	yield %			
1	1a	3a	1.50	76	0.55	78	1.25	81	0.45	84	1.00	86	0.35	91
		3b	1.00	80	0.30	83	0.35	85	0.20	88	0.15	90	0.10	95
		3c	1.20	79	0.40	81	0.55	84	0.30	86	0.30	89	0.20	94
		3d	1.40	77	0.50	79	1.15	82	0.40	84	0.50	88	0.30	92
		3e	2.15	74	1.05	76	1.50	79	0.55	83	1.25	87	0.45	91
2	1b	3a	2.00	73	1.05	76	1.35	78	0.55	82	1.10	83	0.45	88
		3b	1.10	77	0.40	80	0.45	83	0.30	86	0.20	88	0.20	95
		3c	1.30	75	0.50	78	1.05	81	0.40	83	0.40	86	0.30	92
		3d	1.50	71	1.00	74	1.25	76	0.50	79	1.00	82	0.40	87
		3e	2.25	69	1.15	72	2.00	76	1.05	77	1.35	81	0.55	86
3	1c	3a	2.10	71	1.20	74	1.45	78	1.05	79	1.20	84	0.55	89
		3b	1.20	74	0.50	77	0.55	79	0.40	82	0.30	86	0.30	91
		3c	1.40	72	1.00	75	1.15	77	0.50	80	0.50	82	0.40	87
		3d	2.00	70	1.10	73	1.35	75	1.00	78	1.10	80	0.50	85
		3e	2.35	67	1.25	70	2.10	72	1.15	75	1.45	78	1.05	87
4	1d	3a	2.15	68	1.25	71	1.50	73	1.10	77	1.25	78	1.00	89
		3b	1.25	70	0.55	73	1.00	75	0.45	78	0.35	80	0.35	85
		3c	1.45	67	1.05	70	1.20	72	0.55	74	0.55	79	0.45	88
		3d	2.05	63	1.15	66	1.40	68	1.05	73	1.15	78	0.55	84
		3e	2.45	61	1.30	64	2.15	70	1.20	69	1.50	81	1.10	87

Table 2. Preparation of β -Amino Carbonyl Derivative Catalyst by 4-Nitrobenzyl-Substituted Quaternary Ammonium-Based Pyridinium Salts 2(a–d)

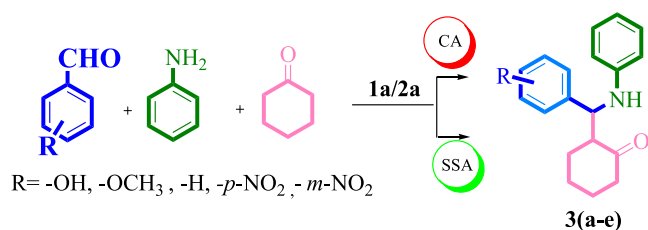
S. No	Catalyst	β -amino carbonyl derivatives	Concentration of 4-nitrobenzyl quaternary ammonium-based pyrazolium salts											
			3.608×10^{-5} mmol				7.217×10^{-5} mmol				1.082×10^{-4} mmol			
			CA		SSA		CA		SSA		CA		SSA	
time (h:m)	yield %	time (h:m)	yield %	time (h:m)	yield %	time (h:m)	yield %	time (h:m)	yield %	time (h:m)	yield %			
1	2a	3a	1.20	81	0.40	87	1.00	90	0.20	93	0.30	93	0.10	95
		3b	0.30	88	0.20	84	0.20	89	0.10	90	0.10	91	0.05	94
		3c	0.50	79	0.25	86	0.30	90	0.13	92	0.15	94	0.07	95
		3d	1.10	81	0.35	90	0.50	93	0.17	95	0.25	94	0.10	97
		3e	1.45	79	0.55	89	1.25	92	0.27	96	0.43	93	0.27	98
2	2b	3a	1.30	85	0.45	85	1.10	89	0.25	91	0.40	92	0.15	96
		3b	0.40	75	0.25	82	0.20	88	0.15	91	0.10	90	0.10	97
		3c	1.00	80	0.30	83	0.40	91	0.18	90	0.25	93	0.12	93
		3d	1.20	73	0.40	89	1.00	91	0.22	93	0.35	93	0.15	96
		3e	1.55	81	1.00	86	1.35	91	0.32	94	0.53	92	0.32	97
3	2c	3a	1.40	73	0.50	82	1.10	86	0.30	90	0.50	91	0.20	94
		3b	0.50	75	0.30	80	0.30	93	0.20	89	0.15	91	0.15	96
		3c	1.00	73	0.35	84	0.50	89	0.23	88	0.35	90	0.17	92
		3d	1.20	80	0.45	88	1.10	89	0.27	92	0.45	91	0.20	93
		3e	1.55	71	1.05	82	1.45	90	0.37	94	1.03	91	0.37	95
4	2d	3a	1.45	73	0.55	80	1.15	84	0.35	89	0.55	90	0.25	90
		3b	0.55	81	0.35	79	0.35	85	0.25	88	0.20	89	0.25	93
		3c	1.05	88	0.40	80	0.55	87	0.28	89	0.45	91	0.22	91
		3d	1.25	79	0.50	86	1.15	88	0.32	91	0.50	90	0.25	92
		3e	2.00	81	1.10	81	1.50	89	0.42	90	1.05	89	0.42	94

interact with the VEGFR-2 kinase receptor *via* π - π stacking and hydrophobic and hydrogen-bonding interactions.

All compounds also displayed many hydrophobic contacts; surprisingly, 2a showed the highest docking score, which was influenced by a hydrogen bond with residue CYS 919, π - π

interaction with ARG 1027, salt bridge LYS 838, and numerous hydrophobic contacts like LEU 840, TYR 927, LEU 1035, PHE 1047, ALA 866, PHE 921, CYC 919, PHE 918, and VAL 848. The effect of noncovalent intermolecular π - π stacking interactions on all molecules is not surprising to show. From

Scheme 3. Synthesis of Substituted Amino Carbonyl Derivatives Using Multiple Methods^a



^aReagent and conditions: CA: CH₃CN, ref, 10–165 min, 80–96%; SSA: Muffle furnace, 100 °C, 05–70 min, 84–98%.

Recycle activity

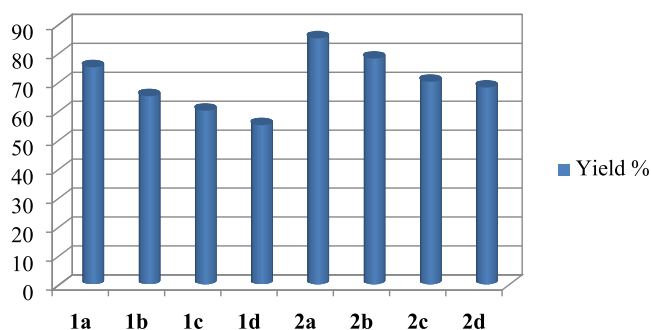


Figure 1. Mannich reaction under recycled substituted quaternary ammonium-based pyridinium salts.

the above facts, compound **2a** strongly binds and regulates the VEGFR-2 kinase activity in therapeutic strategies and cancer prevention (Table 3).

3.2. Physicochemical Properties. A molecular sketcher based on Chem Axon's MarvinJS (<http://www.chemaxon.com>) was used to draw the 2D structure of the molecules to be analyzed. The 2D structures of the designed chemical library have been converted to canonical SMILES format and used to compute the ADME properties in the SwissADME tool.³² The results observed from Table 4 show that the molecular weights of compounds 1–2(a–d) lie below 500 Daltons and thus obey one of the criteria of the Lipinski rule of five. The compounds possess less than 10 rotatable bonds; hence, they satisfy the criterion for oral bioavailability. The PSA is calculated using the fragmental technique called topological polar surface area (TPSA), considering sulfur and phosphorus as polar atoms.³³ This has proved to be a useful descriptor in many models and rules to quickly estimate some ADME properties, especially with regard to biological barrier crossing, such as absorption and brain access.³⁴ It is evident from Table 4 that the TPSA values range from 3.88 to 95.52 Å², whereas the compounds **2a** and **1a** are found to be more polar with TPSA 95.52 Å² and the compounds 1(a–d) have the lowest TPSA value of 3.88 Å².

3.3. Pharmacokinetic Properties. Compounds **2a** and **1a** were observed to have high intestinal absorption except for compounds **1a** and **1d**, which have low GI absorption and high TPSA, and the compounds with high GI absorption could permeate quite easily across the intestinal lining of the cell membrane. Distribution of drugs into the central nervous system (CNS) plays an important role in drug discovery as the CNS lies behind the blood–brain barrier (BBB). Drugs need to pass over the blood–brain barrier (BBB) to reach their target. It is observed from Table 5 that compounds **2a** and **1a** have no BBB

penetration and hence do not affect the CNS. P-glycoprotein (P-gp) plays a key role in keeping nonessential molecules out of the brain and thus has partial permeability.^{35,36} Table 5 shows that all six compounds are substrates of P-gp and all compounds are metabolized by CYP2C19 and CYP1A2. From the log *K_p* values, it is seen that compound **1d** has the least negative value, and thus, it is more skin permeant. Compound **2a** has more negative log *K_p* values and the least is the skin permeant.

3.4. Skin Permeable Model. The total polar surface area (TPSA) values are dependent on skin permeation detection. The more polar the molecule is the less skin permeant. Hence, from Table 6, compounds **2a** and **1a** have TPSA of 95.52 Å², which is found to be less skin permeant, and **2a** and **1a** with TPSA of 3.88 Å² are considered as more skin permeant.

3.5. Boiled Egg Representation. Brain Or Intestinal Estimated permeation method (BOILED-Egg) is the representation of curcumin and Schiff base diol monomers (Figure 4). The BOILED-Egg is the instinctive method to assess passive gastrointestinal absorption (HIA) and brain penetration (BBB) with respect to WLOGP-versus-TPSA.³⁴ The white yolk of the egg is of high probability of passive absorption by the gastrointestinal tract, and the yellow region (yolk) is of high probability of brain penetration. Compounds **2a** and **1a** lie in the white region. The compounds that are nonsubstrates of P-gp are indicated by red dots.

3.6. Bioavailability Radar. The drug-likeness of a molecule can be rapidly assessed from the bioavailability radar (Figure 5). The pink-colored zone is the suitable physicochemical space for oral bioavailability, and the radar plot of the molecule has to fall entirely in the zone to be considered drug-like.³⁷ The pink area represents the optimal range of each property: LIPO (lipophilicity): -0.7 < XLOGP 3 < +5.0; SIZE: 150 g/mol < MW < 500 g/mol; POLAR (polarity): 20 Å² < TPSA < 130 Å²; INSOLU (insolubility): 0 < Log S (ESOL) < 6; INSATU (insaturation): 0.25 < fraction of Csp3 < 1; FLEX (flexibility): 0 < No. of rotatable bonds < 9. From the SwissADME prediction output, it is evident that all compounds were in the optimal range of all of the five properties, except for solubility, enabling them to be considered to possess proficient chemotherapeutic potentials.

4. CONCLUSIONS

Benzyl/4-nitrobenzyl quaternary ammonium-based pyridinium salts are prepared under conventional/solvent-free silica-supported Muffle furnace conditions. The Muffle furnace method is nearly ten times faster than the conventional method. Catalytic studies of benzyl/4-nitrobenzyl pyridinium salts are carried out with different concentrations for the preparation of β-amino carbonyl compound, and it is observed that 4-nitrobenzyl pyridinium salts showed higher catalytic activity than benzyl-substituted pyridinium salts because of their better Lewis character. Even in very low concentrations, it showed potential catalytic activity. Br⁻, PF₆⁻, CF₃SO₃⁻, and BF₄⁻ counter anions containing substituted quaternary ammonium-based pyridinium salts are also tried in the preparation of β-amino carbonyl compound. Among these, the bromide counter anion containing salts showed higher catalytic activity than the other counteranions. Interestingly, candidate **1c** has much more interaction and higher binding affinity with the model protein active site of the VEGFR-2 kinase receptor. Pharmacokinetic studies have taken our compound of interest to the various PBPK models and helped our research to identify the best lead compound. The predicted gastrointestinal absorption of the

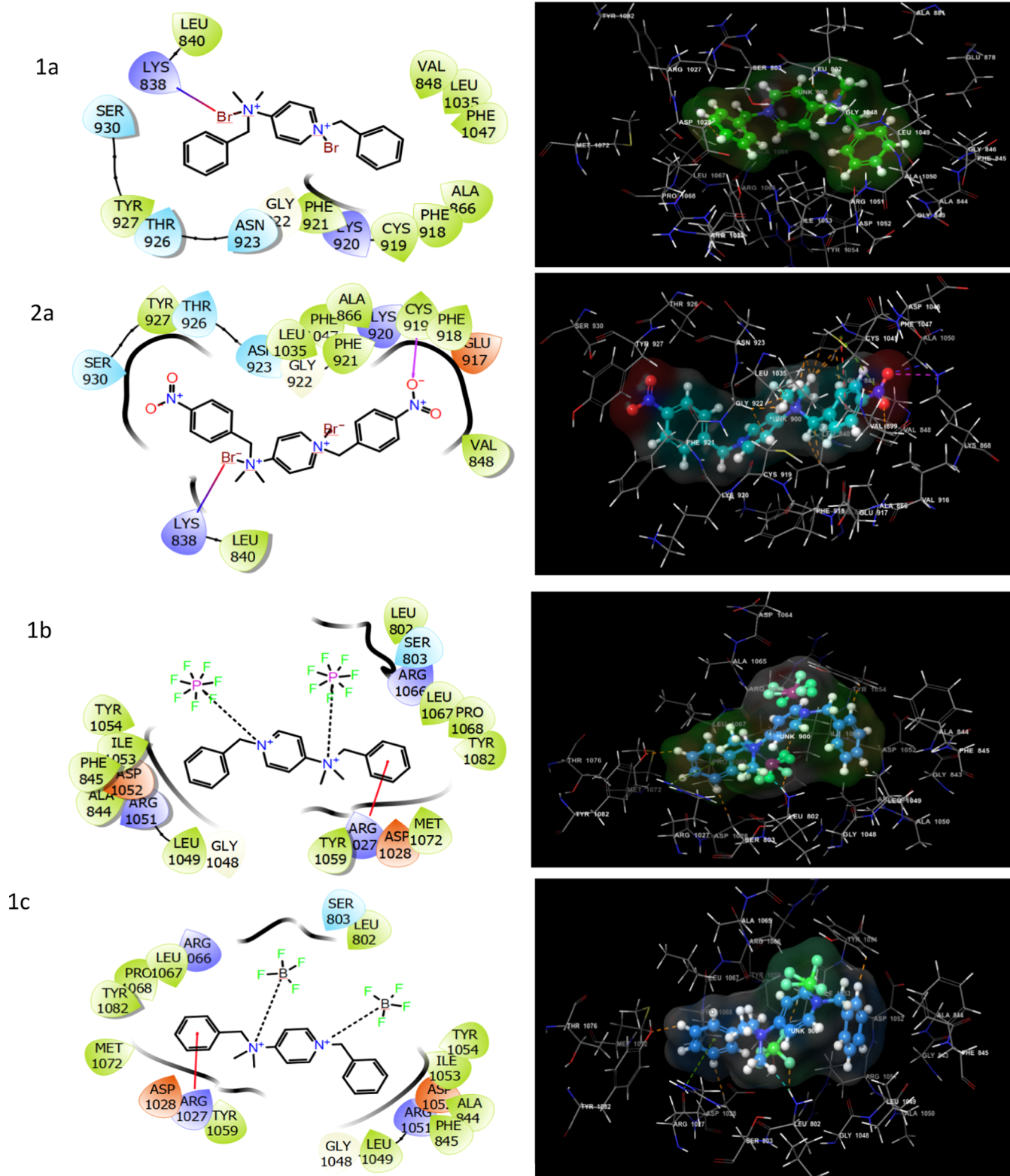


Figure 2. Molecular simulation. 2D and 3D structures of compounds 1a, 2a, 1b, and 1c with the receptor VEGFR-2 kinase.

compounds, bromide counterion-containing compounds, was displayed high and could assess the absence of toxicity at the CNS level due to nonpermeation across the blood–brain barrier. The $\log K_p$ values were found to be optimal and hence are predicted to have good permeability and oral absorption, and the oral bioavailability is found to be universal. This study employed pharmacokinetic research and molecular simulations

to find an intriguing structure to be used as a future drug candidate for human health.

5. EXPERIMENTAL SECTION

5.1. General Procedure for *N,N*-Alkylation Reaction by the Conventional Approach. *N,N*-dimethyl pyridine-4-

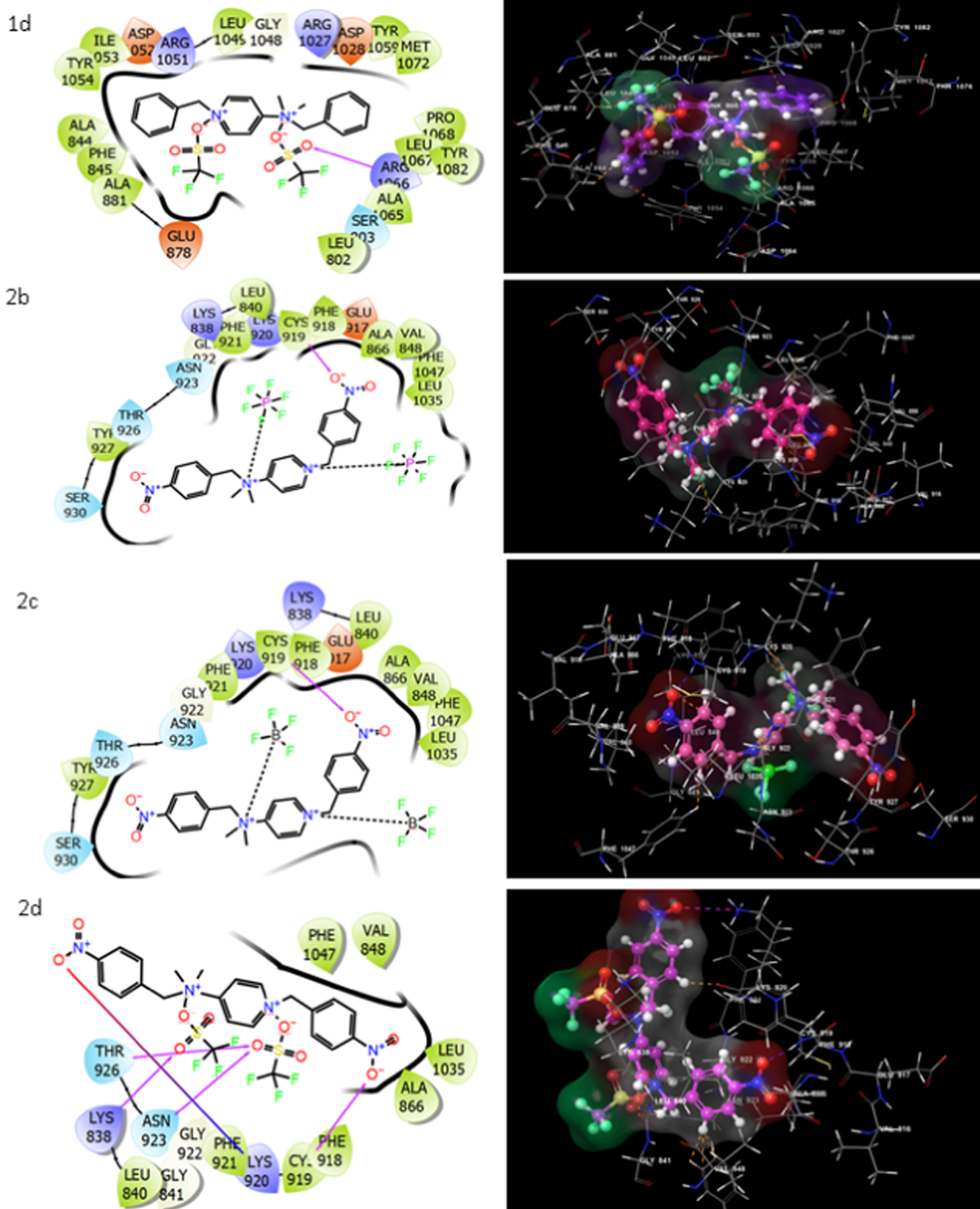


Figure 3. Molecular simulation. 2D and 3D structures of compounds 1a, 2b, 2c, and 2d with the receptor VEGFR-2 kinase.

amine (1.853×10^{-3} mmol; 1.0 equiv) is treated with benzyl/4-nitrobenzyl bromide (1.65×10^{-2} mmol; 2.05 equiv) in the presence of 20 mL of dry acetonitrile under refluxing conditions for 30–45 min. to give *N*-alkylated product of compound 1a/2a.

5.2. General Procedure for *N*-Alkylation Reaction by the Solvent-Free Silica-Supported Approach. Benzyl/4-nitrobenzyl bromide (1.65×10^{-2} mmol; 1.05 equiv) is mixed with required equivalent of *N,N*-dimethyl pyridine-4-amine,

Table 3. Molecular Docking Studies of Compounds 1–2(a–d) with VEGFR-2 Kinase

ionic liquids	docking score kcal·mol ⁻¹	active sites with a mode of interaction			
		H-bond	π - π stacking	salt bridge	hydrophobic contacts (cutoff at 5 Å)
1a	-4.14			LYS 838	LEU 840, TYR 927, PHE 921, CYS 919, PHE 918, ALA 866, VAL 848, LEU 1035, PHE 1047
2a	-6.41	CYS 919		LYS 838	LEU 840, TYR 927, LEU 1035, PHE 1047, ALA 866, PHE 921, CYC 919, PHE 918, VAL 848
1b	-4.34	ARG 1027			TYR 1054, ILE 1053, PHE 845, ALA 844, LEU 1049, TYR 1059, MET 1072, TYR 1082, PRO 1068, LEU 1067, LEU 802
1c	-4.15	ARG 1027			LEU 802, LEU 1067, PRO 1068, TYR 1082, TYR 1059, LEU 1049, PHE 845, ALA 944, ILE 1053, TYR 1054
1d	-5.742	ARG 1066			LEU 802, ALA 1065, LEU 1067, TYR 1082, PRO 1068, MET 1072, TYR 1059, LEU 1045, ILE 1049, ILE 1053, TYR 844, PHE 845, ALA 881
2b	-4.571	CYS 919			TYR 927, PHE 921, LEU 840, CYS 919, PHE 918, ALA 866, VAL 848, PHE 1047, LEU 1035
2c	-4.678	CYS 919			TYR 927, PHE 921, CYS 919, PHE 918, LEU 840, ALA 866, VAL 848, PHE 1047, LEU 1035
2d	-5.927	LYS 838 ASN 923 THR 926		LYS 920	PHE 1047, VAL 848, LEU 1035, ALA 866, PHE 918, CYS 919, PHE 921, LEU 849

Table 4. Physicochemical Properties

monomers	MW	TPSA	#rotatable bonds	ESOL class
M1	464.24	3.88	5	poorly soluble
M2	554.23	95.52	7	poorly soluble
M4	479.05	3.88	5	poorly soluble
M7	569.04	95.52	7	poorly soluble

followed by fine grinding with 5 g of silica gel (60–120 mesh) and kept in a Muffle furnace at 100 °C (optimized temperature) for 10–15 min to afford desired products of compound 1a/2a in quantitative yield.

5.2.1. 1-Benzyl-4-[benzyl (dimethyl) azaniumyl]pyridine-1-ium Bromide (1a). Yield: 1.0 g (86%), Liquid; ¹H NMR: (400 MHz, DMSO-*d*₆) δ : 3.75 (s, 6H), 4.78 (s, 2H), 5.65 (s, 2H), 7.56–7.72 (m, 10H), 8.17–8.25 (d, 4H). ¹³C NMR: (100 MHz, DMSO-*d*₆) δ : 32.4, 58.6, 62.4, 123.5, 124.1, 130.9, 143.3, 145.9 and 146.7. MS (FAB): *m/z* 464.24 [M]⁺; Anal. Calcd. for C₂₁H₂₄Br₂N₂: C: 54.33; H: 5.21; N: 6.03; Found: C: 54.28; H: 5.16; N: 5.98.

5.2.2. 1-Nitrobenzyl-4-[nitrobenzyl (dimethyl) azaniumyl]pyridine-1-ium Bromide (2a). Yield: 1.0 g (86%); Liquid; ¹H NMR: (400 MHz, DMSO-*d*₆) δ : 3.85 (s, 6H), 4.47 (s, 2H), 5.60 (s, 2H), 6.91–7.41 (m, 8H), 8.61–8.63 (d, 4H); ¹³C NMR: (100 MHz, DMSO-*d*₆) δ : 33.6, 40.5, 60.7, 108.4, 128.7, 129.2, 134.2, 137.7 and 142.6; MS (FAB): *m/z* 554.23 [M]⁺; Anal. Calcd. for C₂₁H₂₂Br₂N₄O₄: C: 45.51; H: 4.00; N: 10.11. Found: C: 45.46; H: 3.96; N: 7.57.

5.3. General Procedure for Anion Exchange Reaction. Simple/substituted pyridinium bromide 1a/2a (1.705 × 10⁻³ mmol; 1.0 equiv) is treated with various counteranions containing inorganic salts, such as NaBF₄, K₄PF₆, and LiCF₃SO₃ (3.496 × 10⁻³ mmol; 2.05 equiv), in 20 mL of deionized water at room temperature with stirring for 2 h to give an anion exchange product of compounds 1–2(b–d) in 90–97% yield. Both metallic bromide and pyridinium salts are soluble in water. So,

Table 5. Pharmacokinetic Properties

monomers	GI absorption	BBB permeant	P-gp substrate	log K _p (cm/s)	CYP2C19 inhibitor	CYP1A2 inhibitor
M1	low	Yes	No	-4.92	No	No
M2	high	No	No	-5.71	Yes	No
M4	low	Yes	No	-3.24	No	No
M7	high	No	No	-4.03	No	No

Table 6. Skin Permeable Model

molecule	TPSA	log K _p (cm/s)
1	3.88	-4.92
2	95.52	-5.71
4	3.88	-3.24
7	95.52	-4.03

separation is not easier under these circumstances, and Soxhlet extraction is used for separation with dry THF for 2 h reflux. An anion exchange reaction is confirmed by an aqueous AgNO₃ solution.

5.3.1. 1-Benzyl-4-[benzyl (dimethyl) azaniumyl]pyridine-1-ium Hexafluorophosphate (1a). Yield: 0.5 g (84%); Liquid; ¹H NMR: (400 MHz, DMSO-*d*₆) δ : 3.73 (s, 6H), 4.76 (s, 2H), 5.63 (s, 2H), 7.54–7.70 (m, 10H), 8.15–8.23 (d, 4H); ¹³C NMR: (100 MHz, DMSO-*d*₆) δ : 32.2, 58.4, 62.2, 123.3, 123.9, 130.7, 143.1, 145.7 and 146.5; MS (FAB): *m/z* 594.36 [M]⁺; Anal. Calcd. for C₂₁H₂₄F₁₂N₂P₂: C: 42.44; H: 4.07; N: 4.71; Found: C: 42.39; H: 4.03; N: 4.69.

5.3.2. 1-Benzyl-4-[benzyl (dimethyl) azaniumyl]pyridine-1-ium Tetrafluoroborate (1b). Yield: 0.5 g (94%); Liquid; ¹H NMR: (400 MHz, DMSO-*d*₆) δ : 3.72 (s, 6H), 4.75 (s, 2H), 5.62 (s, 2H), 7.53–7.69 (m, 10H), 8.14–8.22 (d, 4H); ¹³C NMR: (100 MHz, DMSO-*d*₆) δ : 32.1, 58.3, 62.1, 123.2, 123.8, 130.1, 143.0, 145.6, and 146.4; MS (FAB): *m/z* 478.04 [M]⁺; Anal. Calcd. for C₂₁H₂₄B₂F₈N₂: C: 52.76; H: 5.06; N: 5.86; Found: C: 52.71; H: 5.02; N: 5.85.

5.3.3. 1-Benzyl-4-[benzyl (dimethyl) azaniumyl]pyridine-1-ium Trifluoromethanesulfonate (1c). Yield: 0.3 g (95%); Liquid; ¹H NMR: (400 MHz, DMSO-*d*₆) δ : 3.71 (s, 6H), 4.74 (s, 2H), 5.61 (s, 2H), 7.52–7.68 (m, 10H), 8.13–8.21 (d, 4H); ¹³C NMR: (100 MHz, DMSO-*d*₆) δ : 32.0, 58.2, 62.0, 123.1, 123.7, 130.0, 142.9, 145.5 and 146.3; MS (FAB): *m/z* 602.57 [M]⁺; Anal. Calcd. for C₂₃H₂₄F₆N₂O₆S₂: C: 45.84; H: 4.01; N: 4.65; Found: C: 45.80; H: 3.98; N: 4.64.

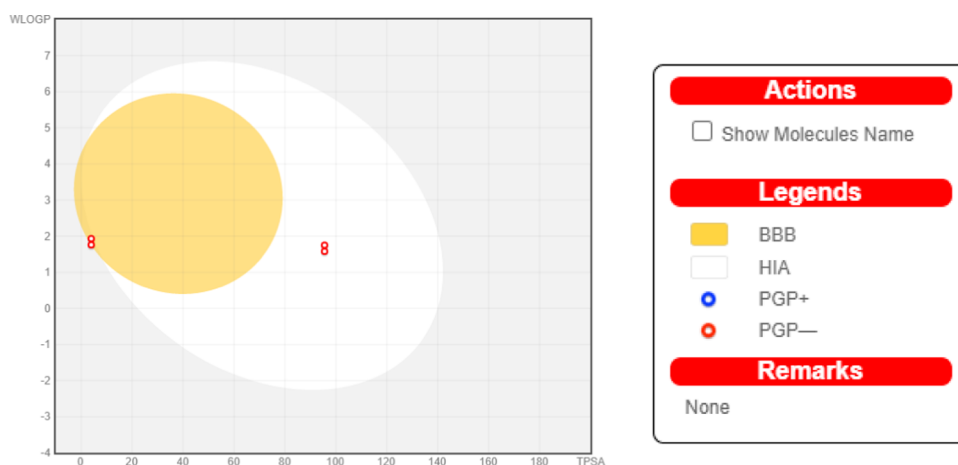


Figure 4. Boiled egg representation.

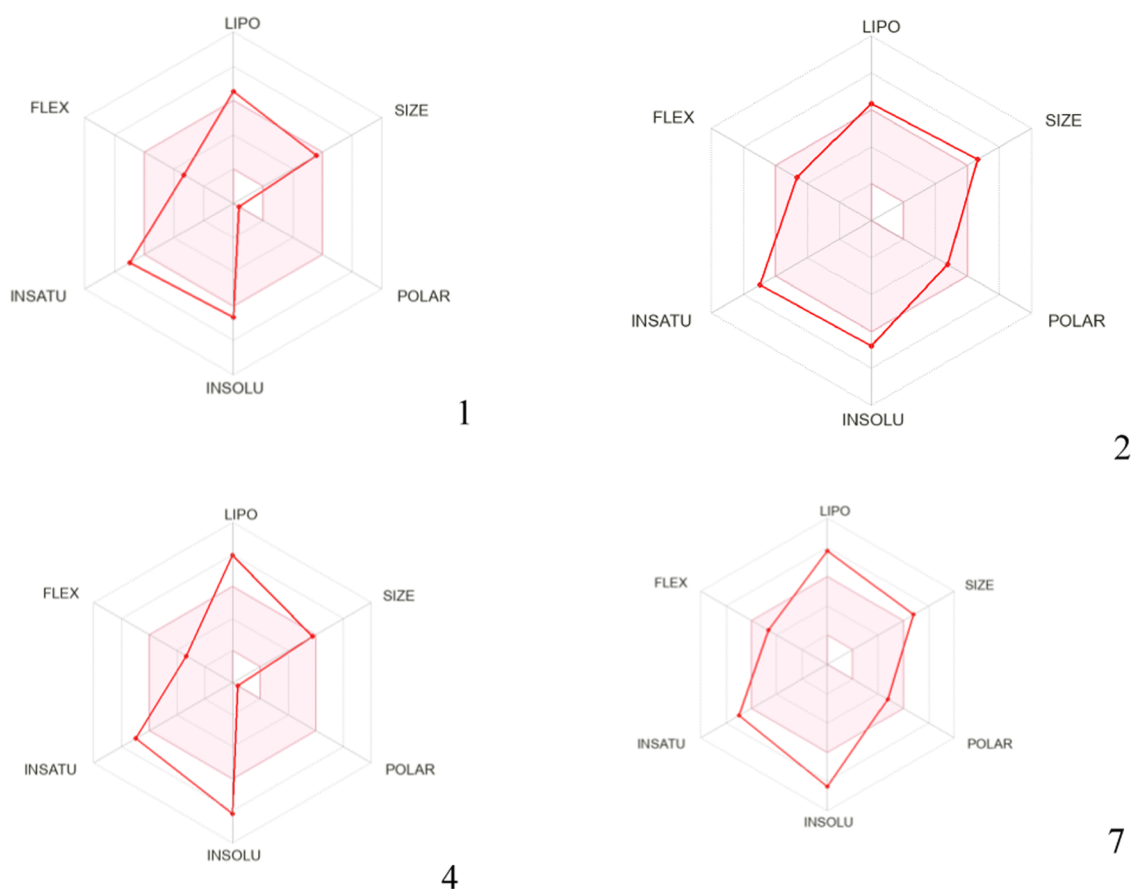


Figure 5. Bioavailability radar.

5.3.4. 1-Nitrobenzyl-4-[nitrobenzyl (dimethyl) azaniumyl]-pyridine-1-ium Hexafluorophosphate (2a). Yield: 0.3 g (93%); Liquid; ^1H NMR: (400 MHz, $\text{DMSO-}d_6$) δ : 3.83 (s, 6H), 4.45 (s, 2H), 5.58 (s, 2H), 6.89–7.38 (m, 8H), 8.59–8.62 (d, 4H); ^{13}C NMR: (100 MHz, $\text{DMSO-}d_6$) δ : 33.4, 40.3, 60.5, 108.2, 128.5, 129.0, 134.0, 137.5, 142.4; MS (FAB): m/z 684.35 $[\text{M}]^+$; Anal. Calcd. for $\text{C}_{21}\text{H}_{22}\text{F}_{12}\text{N}_4\text{O}_4\text{P}_2$; C: 36.86; H: 3.24; N: 8.19; Found: C: 36.82; H: 3.21; N: 8.18.

5.3.5. 1-Nitrobenzyl-4-[nitrobenzyl (dimethyl) azaniumyl]-pyridine-1-ium Tetrafluoroborate (2b). Yield: 0.3 g (96%); Liquid; ^1H NMR: (400 MHz, $\text{DMSO-}d_6$) δ : 3.82 (s, 6H), 4.44 (s, 2H), 5.57 (s, 2H), 6.88–7.37 (m, 8H), 8.58–8.61 (d, 4H);

^{13}C NMR: (100 MHz, $\text{DMSO-}d_6$) δ : 33.3, 40.2, 60.4, 108.1, 128.4, 128.9, 133.9, 137.4, 142.3; MS (FAB): m/z 568.03 $[\text{M}]^+$; Anal. Calcd. for $\text{C}_{21}\text{H}_{22}\text{B}_2\text{F}_8\text{N}_4\text{O}_4$; C: 54.33; H: 5.21; N: 6.03; Found: C: 54.28; H: 5.16; N: 5.98.

5.3.6. 1-Nitrobenzyl-4-[nitrobenzyl (dimethyl) azaniumyl]-pyridine-1-ium Trifluoromethanesulfonate (2c). Yield: 0.3 g (97%); Liquid; ^1H NMR: (400 MHz, $\text{DMSO-}d_6$) δ : 3.81 (s, 6H), 4.43 (s, 2H), 5.56 (s, 2H), 6.87–7.36 (m, 8H), 8.57–8.60 (d, 4H); ^{13}C NMR: (100 MHz, $\text{DMSO-}d_6$) δ : 33.2, 40.1, 60.3, 108.0, 128.3, 128.8, 133.8, 137.3, 142.2; MS (FAB): m/z 692.56 $[\text{M}]^+$; Anal. Calcd. for $\text{C}_{23}\text{H}_{22}\text{F}_6\text{N}_4\text{O}_{10}\text{S}_2$; C: 39.89; H: 3.20; N: 8.09; Found: C: 39.85; H: 3.17; N: 8.08.

5.4. General Procedure for the Synthesis of β -Amino Carbonyl Derivatives. Equal molar concentration of substituted aryl aldehyde (3.28×10^{-3} mmol; 1.0 equiv) is mixed with aniline (3.45×10^{-3} mmol; 1.05 equiv) and cyclohexanone (3.45×10^{-3} mmol; 1.05 equiv), and optimized concentration of catalyst benzylated pyridinium bromide **2a** (5.44×10^{-5} mmol) is added in the presence of CH_3CN under reflux for 10–165 min to give quinoline derivative of compounds **3(a–e)** in 67–96%.

5.4.1. 2-(Phenyl (phenylamino) methyl) cyclohexanone (3a). Yield: 0.5 g (91%); mp: 104–106 °C; ^1H NMR: (400 MHz, $\text{DMSO}-d_6$) δ : 1.63–1.73 (m, 2H), 1.80–1.96 (m, 4H), 2.29–2.48 (m, 2H), 2.75–2.85 (m, 1H), 4.61 (d, 1H), 6.56 (dd, 2H), 6.65 (t, 1H), 7.04–7.10 (m, 2H), 7.17–7.24 (m, 1H), 7.27–7.33 (m, 2H), 7.33–7.41 (m, 2H); ^{13}C NMR: (100 MHz, $\text{DMSO}-d_6$) δ : 31.2, 41.7, 42.3, 57.2, 58.0, 113.6, 114.0, 117.5, 126.9, 127.2, 128.3, 129.0, 141.5, 147.4 and 212.8. MS (FAB): m/z 279.3 [M] $^+$; Anal. Calcd for $\text{C}_{19}\text{H}_{21}\text{NO}$; C: 81.68; H: 7.58; N: 5.01; Found: C: 81.65; H: 7.49; N: 4.98.

■ ASSOCIATED CONTENT

Supporting Information

The Supporting Information is available free of charge at <https://pubs.acs.org/doi/10.1021/acsomega.2c07129>.

Characterization data for **1a** and **2a** (PDF)

■ AUTHOR INFORMATION

Corresponding Author

Kilivelu Ganesan – PG & Research Department of Chemistry, Presidency College (Autonomous), Chennai 600005, India; orcid.org/0000-0003-2127-4388; Email: kiliveluganesan@yahoo.co.in

Authors

Ramalingam Tamilarasan – PG & Research Department of Chemistry, Presidency College (Autonomous), Chennai 600005, India; Department of Chemistry, Vel Tech Multi Tech Dr. Rangarajan Dr. Sakunthala Engineering College (Autonomous), Chennai 600062, India

Annadurai Subramani – Department of chemistry, Apollo Arts and Science College, Poonamallee, Chennai, Tamil Nadu 60210, India

Liyakath Benazir Ali – PG and Research Department of Chemistry, The New College, Chennai 60014, India

Mohammed Mujahid Alam – Department of Chemistry, College of Science, King Khalid University, Abha 61413, Kingdom of Saudi Arabia

Amanullah Mohammed – Department of Clinical Biochemistry, College of Medicine, King Khalid University, Abha 61413, Kingdom of Saudi Arabia

Complete contact information is available at <https://pubs.acs.org/doi/10.1021/acsomega.2c07129>

Notes

The authors declare no competing financial interest.

■ ACKNOWLEDGMENTS

M.M.A. and M.A. thank the Deanship of Research, King Khalid University, Saudi Arabia for Small Research Group under the grant number R.G.P. 1/339/1443.

■ REFERENCES

- Smiglak, M.; Metlen, A.; Rogers, R. D. The second evolution of ionic liquids: from solvents and separations to advanced materials energetic examples from the ionic liquid cookbook. *Acc. Chem. Res.* **2007**, *40*, 1182.
- Dupont, J.; Souza, R. F.; Suarez, P. A. Z. Ionic liquid (molten salt) phase organometallic catalysis. *Chem. Rev.* **2002**, *102*, 3667.
- van Rantwijk, F.; Sheldon, R. A. Biocatalysis in ionic liquids. *Chem. Rev.* **2007**, *107*, 2757.
- Martins, M. A. P.; Frizzo, C. P.; Moreira, D. N. N.; Zanatta Bonacorso, H. G.; Bonacorso, H. G. Ionic liquids in heterocyclic synthesis. *Chem. Rev.* **2008**, *108*, 2015.
- Olivier-Bourbigou, H.; Magna, L.; Morvan, D. Ionic liquids and catalysis: Recent progress from knowledge to applications. *Appl. Catal., A* **2010**, *373*, 1.
- Nitulescu, G. M.; Draghici, C.; Missir, A. V. Synthesis of new pyrazole derivatives and their anticancer evaluation. *Eur. J. Med. Chem.* **2010**, *45*, 4914.
- Ly, P.-C.; Li, H. Q.; Sun, J. A.; Zhou, Y.; Zhu, H. L. Synthesis and biological evaluation of pyrazole derivatives containing thiourea skeleton as anticancer agents. *Bioorg. Med. Chem.* **2010**, *18*, 4606.
- Tokuda, H.; Hayamizu, K.; Ishii, K.; Susan, M. A. B. H.; Watanabe, M. Physicochemical properties and structures of room temperature ionic liquids. 2. Variation of alkyl chain length in imidazolium cation. *J. Phys. Chem. A* **2004**, *108*, 16593.
- Baltus, R. E.; Counce, R. M.; Culbertson, B. H.; Luo, H.; DePaoli, D. W.; Dai, S.; Duckworth, D. C. Examination of the potential of ionic liquids for gas separations. *Sci. Technol.* **2005**, *40*, 525.
- Shi, W.; Sorescu, D. C.; Luebke, D. R.; Keller, M. J.; Wickramanayake, J. Molecular simulations and experimental studies of solubility and diffusivity for pure and mixed gases of H_2 , CO_2 , and Ar absorbed in the ionic liquid 1-*n*-hexyl-3-methylimidazolium bis(trifluoromethylsulfonyl) amide ([hmim][Tf₂N]). *J. Phys. Chem. B* **2010**, *114*, 6531.
- Zhang, Q.; Zhang, S.; Deng, Y. Recent advances in ionic liquid catalysis. *Green Chem.* **2011**, *13*, 2619.
- Tokuda, H.; Hayamizu, K.; Ishii, K.; Susan, M. A. B. H.; Watanabe, M. Physicochemical properties and structures of room temperature ionic liquids. 2. Variation of alkyl chain length in imidazolium cation. *J. Phys. Chem. B* **2005**, *109*, 6103.
- Nulwala, H. B.; Tang, C. N.; Kail, B. W.; Damodaran, K.; Kaur, P.; Wickramanayake, S.; Shic, W.; Luebke, D. R. Probing the structure-property relationship of regioisomeric ionic liquids with click chemistry. *Green Chem.* **2011**, *13*, 3345.
- Mohy El-Din, M. M.; Senbel, A. M.; Bistawroos, A. A.; El-Mallah, A.; El-Din, N. A. N.; Bekhit, A. A.; Abd El Razik, H. A. A. A novel COX-2 inhibitor pyrazole derivative proven effective as an anti-inflammatory and analgesic drug. *Besic Clin. Pharmacol.* **2011**, *108*, 263.
- Boschi, D.; Guglielmo, S.; Aiello, S.; Morace, G.; Borghi, E.; Fruttero, R. Synthesis and *in vitro* antimicrobial activities of new (cyano-NNO-azoxy) pyrazole derivatives. *Bioorg. Med. Chem. Lett.* **2011**, *21*, 3431.
- Souza, F. R.; Souza, V. T.; Ratzlaff, V.; Borges, L. P.; Oliveira, M. R.; Bonacorso, H. G.; Zanatta, N.; Martins, M. A. P.; Mello, C. F. Hypothermic and antipyretic effects of 3-methyl and 3-phenyl-5-hydroxy-5-trichloromethyl-4, 5-dihydro-1H-pyrazole-1-carboxyamides in mice. *Eur. J. Pharmacol.* **2002**, *451*, 141.
- Ningning, Z. Y.; Xinying, Z. L.; Fan, X. Regio- and chemoselective mono- and bisnitration of 8-amino quinoline amides with $\text{Fe}(\text{NO}_3)_3 \cdot 9\text{H}_2\text{O}$ as promoter and nitro source, *Org. Lett.*, **2016**, *18*, 6054. DOI: [10.1021/acscorglett.6b02998](https://doi.org/10.1021/acscorglett.6b02998).
- Carmichael, A. J.; Earle, M. J.; Holbrey, J. D.; McCormac, P. B.; Seddon, K. R. The Heck reaction in ionic liquids: a multiphasic catalyst system. *Org. Lett.* **1999**, *1*, 997.
- (a) Ganapathi, P.; Ganesan, K.; Mahendiran, D.; Alam, M. M.; Amanullah, M. Efficient Antibacterial dimeric nitro imidazolium type of ionic liquids from a simple synthetic approach. *ACS Omega* **2022**, *7*, 44458. (b) Tamilarasan, R.; Ganesan, K. A Facile and solvent-free silica-supported route for the preparation of pyrazolium salts and its catalytic

response. *J. Heterocyclic Chem.* **2017**, *54*, 2817. (c) Xu, L.; Chen, W.; Xiao. Heck reaction in ionic liquids and the insitu identification of N-heterocyclic carbene complexes of palladium. *J. Organometallics* **2000**, *19*, 1123. (d) Manikandan, C.; Ganesan, K. Silica-supported solvent approaches more facile than the conventional for Erlenmeyer synthesis with our pyridinium salts. *J. Heterocyclic Chem.* **2018**, *55*, 929.

(20) (a) Ganesan, K.; Alias, Y. Synthesis and characterization of novel dimeric ionic liquids from conventional approach. *Int. J. Mol. Sci* **2008**, *9*, 1207. (b) Ganapathi, P.; Ganesan, K. Synthesis and characterization of 1,2-dimethyl imidazolium type of ionic liquids and its catalytic activities. *Syn. Commun.* **2015**, *45*, 2135. (c) Ganapathi, P.; Ganesan, K. Synthesis and characterization of methyl substituted imidazolium dimeric ionic liquids and their catalytic activities. *Am. J. Chem. & Appl.* **2014**, *1*, 40.

(21) (a) Ganapathi, P.; Ganesan, K.; Vijaykanth, N.; Arunagirinathan, N. Anti-bacterial screening of water-soluble carbonyl diimidazolium salts and its derivatives. *J. Mol. Liq.* **2016**, *219*, 180. (b) Tamilarasan, R.; Govindaraj, S.; Ganesan, K. Synthesis of dimeric pyridinium bromide under silica supported approach. *Syn. Commun.* **2020**, *50*, 1190. (c) Ganapathi, P.; Ganesan, K. Synthesis and characterization of 1, 2-dimethyl imidazolium ionic liquids and their catalytic activities. *Syn. Commun.* **2015**, *45*, 2135.

(22) Manikandan, C.; Ganesan, K. Synthesis, characterization, and catalytic behavior of methoxy-and dimethoxy-substituted pyridinium-type ionic liquids. *Syn. Commun.* **2014**, *44*, 3362.

(23) (a) Manikandan, C.; Ganesan, K. Solid-supported synthesis of flexible dimeric pyridinium salts and their catalytic activities. *Syn. Lett.* **2016**, *27*, 1527. (b) Ganapathi, P.; Ganesan, K. Anti-bacterial, catalytic and docking behaviours of novel di/trimeric imidazolium salts. *J. Mol. Liq.* **2017**, *233*, 452. (c) Ramanathan, N.; Ganapathi, P.; Ganesan, K. Silica supported and conventional approaches for the synthesis of carbonyldiimidazole type of ionic liquids and its catalytic activities. *J. Heterocycl. Chem.* **2017**, *54*, 51.

(24) Manikandan, C.; Ganesan, K. Synthesis and characterization of hydroxy substituted pyridinium type of ionic liquids via conventional/silica supported approaches and their applications. *J. Heterocycl. Chem.* **2017**, *54*, 503.

(25) Hay, M.; Thomas, D. W.; Craighead, J. L. Clinical development success rates for investigational. *Nat. Biotechnol.* **2014**, *32*, 40.

(26) Pernak, J.; Rogoz, J.; Mirska, I. Synthesis and antimicrobial activities of new pyridinium and benzimidazolium chlorides. *Eur. J. Med. Chem.* **2001**, *36*, 313.

(27) Roy, B.; Bar, A.; Gole, B.; Mukherjee, P. S. Fluorescent tris-imidazolium sensors for picric acid explosive. *J. Org. Chem.* **2013**, *78*, 1306.

(28) Ghosh, K.; Avik Ranjan, S.; Tanmay, S.; Santanu, P.; Debasis, K. Progress of 3-aminopyridinium-based synthetic receptors in anion recognition. *RSC Adv.* **2014**, *4*, 20114.

(29) Subramaniam, P.; Sharifah, M.; Yatimah, A. Synthesis and characterization of the inclusion complex of dicationic ionic liquid and β -cyclodextrin. *Int. J. Mol. Sci.* **2010**, *11*, 3675.

(30) Chang, T.; Leqin, H.; Li, B.; Haiyan, H.; Mingxia, Y.; Xiaorui, G. Brønsted acid-surfactant-combined catalyst for the mannich reaction in water. *RSC Adv.* **2014**, *4*, 727.

(31) Senapak, W.; Saeeng, R.; Sirion, U. Acid-ionic polymer as recyclable catalyst for one-pot three-component mannich reaction. *RSC Adv.* **2017**, *7*, 30380.

(32) Daina, A.; Michielin, O.; Zoete, V. Swiss ADME: a free web tool to evaluate pharmacokinetics, drug-likeness and medicinal chemistry friendliness of small molecules. *Sci. Rep.* **2017**, *7*, No. 42717.

(33) Ertl, P.; Rohde, B.; Selzer, P. Fast calculation of molecular polar surface area as a sum of fragment-based contributions and its application to the prediction of drug transport properties. *J. Med. Chem.* **2000**, *43*, 3714.

(34) Daina, A.; Zoete, V. A boiled-egg to predict gastrointestinal absorption and brain penetration of small molecules. *Chem. Med. Chem.* **2016**, *11*, 1117.

(35) Liu, X.; Testa, B.; Fahr, A. Lipophilicity and its relationship with passive drug permeation. *Pharm. Res.* **2011**, *28*, 962.

(36) Krämer, S. D.; Wunderli-Allenspach, H. Physicochemical properties in pharmacokinetic lead optimization. *II Farmaco* **2001**, *56*, 145.

(37) Ritchie, T. J.; Ertl, P.; Lewis, R. L. The graphical representation of ADME-related molecule properties for medicinal chemists. *Drug Discovery Today* **2011**, *16*, 65.